JOURNAL OF AGRICULTURAL AND FOOD CHEMISTRY

Article

pubs.acs.org/JAFC

Synthesis, Characterization, and Aqueous Self-Assembly of Octenylsuccinate Oat β-Glucan

Jia Liu,[†] Jing Li,[†] Yaqin Ma,[†] Fang Chen,[†] and Guohua Zhao*[,†,‡]

[†]College of Food Science, Southwest University, Chongqing 400715, P.R. China

[‡]Food Engineering and Technology Research Centre of Chongqing, Chongqing 400715, P.R. China

ABSTRACT: Amphiphilic oat β-glucan derivatives carrying octenylsuccinic groups as hydrophobic moieties have been synthesized. Materials with a different degree of substitution (DS) and weight-average molecular weight (M_w) for oat β-glucan were prepared and characterized using elemental analysis, infrared (IR) spectroscopy, and high performance size exclusion chromatography (HPSEC). Dynamic light scattering (DLS), fluorescence spectroscopy, and transmission electron microscopy (TEM) revealed that octenylsuccinate oat β-glucan (OSG) can self-assemble into spherical micelles in water with an average size ranging from 175 to 600 nm. OSG micelles were negatively charged as indicated by ζ-potential measurement. The critical micelle concentration (CMC) of OSGs varied from 0.206 to 0.039 mg/mL, depending on the DS and M_w of the oat β-glucan. It was found that the presence of OSG micelles in aqueous solution could significantly enhance the solubility of curcumin by 880 fold. Thus, OSG might have great potential in applications as hydrophobic nutrient delivery carriers.

KEYWORDS: *octenylsuccinate oat β-glucan, self-assembly, curcumin*

INTRODUCTION

Self-assembly is an autonomous and spontaneous process that organizes components into ordered or functional structures.[1] Amphiphilic molecules, such as surfactants or lipids, can spontaneously self-assemble in water to form self-aggregates such as micelles, tubes, and vehicles.[2] The formation of micellelike aqueous self-assemblies with a hydrophobic core and hydrophilic shell depends on the repelling and coordinating forces between the hydrophilic and hydrophobic parts of amphiphiles.[3] These self-assemblies are versatile tools in pharmacy, food, and daily chemical industries and are capable of trapping hydrophobic pharmaceuticals and active ingredients in their core. This characteristic increases the stability, solubility/dispersity, and bioavailability of such trapped ingredients.[4−6] Amphiphile self-assemblies can also be used as vehicles for the target delivery and controlled release of bioactive compounds.[7,8] Size and stability are the two most important physicochemical properties of amphiphile self-assemblies. Size is responsible for drug-loading capacity, solubility/dispersity, and bioavailability, whereas stability determines the practical utilization of self-assemblies. Thus, the size and stability of these self-assemblies are highly related to the structural characteristics of amphiphiles and environmental parameters such as temperature, pH, and ionic strength.[9] Studies have revealed that increasing temperature may cause larger micellar growth while the addition of H^+ and salt increases the ionic strength and reduces the thickness of the electric double layer so that there is insufficient repulsive force to stabilize colloidal particles.[10]

Both micro- and macroamphiphiles have the capacity to form self-assemblies in water. Only intermolecular self-assembly occurs spontaneously beyond the critical micelle concentration (CMC) of microamphiphiles. Intramolecular self-assembly occurs within the CMC of microamphiphiles, while intermolecular self-assembly occurs beyond the CMC of macroamphiphiles. In contrast to small amphiphiles, macroamphiphiles can form self-assemblies and maintain stability in dilute solutions.[11]

Polysaccharides, which are the most widely available biomacromolecules, have attracted increasing attention as substrates in forming functional self-assemblies. Given the strong hydrophilicity of polysaccharides, chemical modification is necessary before aqueous self-assembly to endow soluble polysaccharide with hydrophobicity. Starch, chitosan, cellulose, and dextrin modified with fatty acid, oleoyl chloride, 3-chloro-2-hydroxypropyltrimethylammonium chloride, and hexadecanethiol exhibit self-assembly capacities in aqueous media.[12−15] Tea catechin-loaded nanoparticles prepared from chitosan were designed for oral administration of oxidation-sensitive compounds.[16] Alginate−chitosan−pluronic composite nanoparticles were prepared and used to encapsulate curcumin for delivery to cancer cells.[17] Hydrophobically modified sulfated chitosan was prepared and used as a carrier of doxorubicin.[18] Bioactive polysaccharides have been the research focus in pharmaceutical, food, and nutrition fields over the past decades. To our knowledge, few studies have investigated the application of bioactive polysaccharides as substrates in the formation of functional self-assemblies.

The hydrophobic modification of polysaccharides and their self-assembly have been extensively studied, but the previous reports indicated that the self-assembly behavior of polysaccharide-based micelles is highly related to the structure of the substrates. Soluble β-glucan, as a functional and bioactive polysaccharide, consists of linear chains of β-D-glucopyranosyl units linked by (1→3) and (1→4) linkages.[19] Soluble β-glucan

Received: August 9, 2013
Revised: December 8, 2013
Accepted: December 9, 2013
Published: December 9, 2013

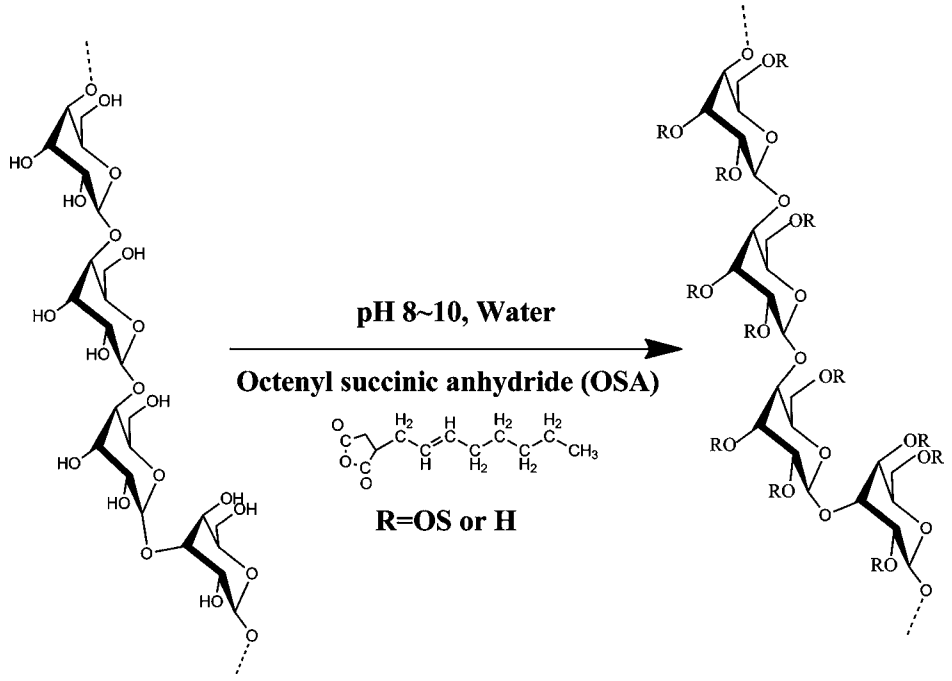

Figure 1. Preparation of octenylsuccinate oat β-glucan (OSG).

improves the immune system, exhibits anticancer activity, and reduces blood cholesterol, lipid, and blood glucose. However, the hydrophobic modification of β-glucan is still lacking. Considering that starch molecules modified with succinic groups are widely applied in the food industry, esterification by octenylsuccination was adopted to prepare hydrophobic oat β-glucan (Figure 1) with regard to safety. Dynamic light scattering (DLS), transmission electron microscopy (TEM), and fluorescence spectroscopy were conducted to investigate intensively the aqueous self-assembly behavior of octenylsuccinate oat β-glucan (OSG). The influences of OSG concentration, pH, and ionic strength on the micelle stability were investigated. Besides, the potential of OSG self-assemblies to enhance the water solubility of curcumin was also verified.

EXPERIMENTAL SECTION

Materials. A commercial soluble β-glucan (80 wt % β-glucan content) extracted from oats was bought from Zhangjiakou Yikang Biological Technology Co., Ltd. (China). 2-Octen-1-ylsuccinic anhydride (product no. 416487) and pyrene (for fluorescence, ≥99.0%, product no. 82648) were purchased from Sigma Chemical Co. (St. Louis, MO). Curcumin (98%) was supplied by Adamas Reagent Co., Ltd. (China). KBr of infrared (IR) spectroscopy grade was obtained from Guangfu Reagent Chemical Co., Ltd. (China). Phosphotungstic acid (>98%) was provided by Sangon Biological Technology Co., Ltd. (China). Acetonitrile and formic acid of chromatographic grade were also used. All chemicals were used in this study without further purification.

Oat β-Glucan Solution. Oat β-glucan (2.500 g) was dispersed in 1 L of distilled water and was heated at 80 °C with magnetic stirring for 2 h. The resulting solution was cooled to room temperature by tap water. The oat β-glucan solution (1.953 ± 0.075 g of β-glucan) was obtained by centrifugation at 3000*g* for 10 min.

Oat β-Glucan Hydrolysis. The hydrolysis of β-glucan was conducted according to a previously described method with slight modifications.[20] An aliquot of 100 or 200 μL of hydrochloric acid (6 M) was added to 100 mL of β-glucan solution (0.195 ± 0.008 g of β-glucan). After the digestion at 50 °C for 10 min, the hydrolysates (0.192 ± 0.007 g of β-glucan for 100 μL of hydrochloric acid (6 M) and 0.188 ± 0.004 g of β-glucan for 200 μL of hydrochloric acid (6 M)) was rapidly cooled to room temperature and neutralized (pH 6 to pH 7) with 2 M NaOH. A high-performance size exclusion chromatography (HPSEC) system was used to determine the weight-average molecular weight (M_w) of β-glucan and its hydrolyates. The HPSEC system consists of a pump (20 A; Shimadzu, Japan), an autoinjector (20 A; Shimadzu, Japan), a 7.8 mm × 300 mm TSK G4000 PWXL-SEC column (Tosoh, Japan), and a refractive index detector (10 A; Shimadzu, Japan). The flow rate of the mobile phase (0.02% (m/v) NaN_3) was 0.7 mL/min.[21]

OSG Synthesis and Characterization. OSG was synthesized according to a previously proposed method for the octenylsuccination of starch with slight modifications.[22] By varying the amounts of 2-octen-1-ylsuccinic anhydride and incubation time, a series of OSGs with different degrees of substitution (DS) was obtained. An aliquot solution of 100 mL of oat β-glucan (16.8×10^4 g/mol) or its hydrolysates (11.9×10^4 and 7.3×10^4 g/mol) was introduced into a reaction bulb. A 0.3 mL amount of 2-octen-1-ylsuccinic anhydride was added, and the mixture was incubated at 45 °C for 2 h under continuous stirring to obtain OSG1, OSG4, and OSG5, respectively. An aliquot of 100 mL of oat β-glucan (16.8×10^4 g/mol) solution was introduced into a reaction bulb. A 0.6 mL amount of 2-octen-1-ylsuccinic anhydride was added, and the mixture was incubated at 45 °C for 2 and 5 h under continuous stirring to obtain OSG2 and OSG3, respectively. During the reaction, the pH of the mixture was maintained in the range of pH 8 to pH 10 by the dropwise addition of 3.0% (w/v) NaOH. The reaction mixture was then cooled by tap water and was further stirred for 12 h at room temperature. The reaction was ended by adding 0.24 M HCl to obtain a pH of 6.5. The slurry was filtered through a Buchner funnel by using Whatman #l filter paper vacuum filtration. Thereafter, OSG was precipitated from the filtrate by adding isopropyl alcohol up to 66.7% (v/v) isopropyl alcohol concentration. The precipitate was collected by centrifugation at 3000*g* for 10 min. The pellet was dissolved in distilled water and successively dialyzed against tap water and distilled water for 24 h in a dialysis bag (MD44-14, Union Carbide Co., Seadrift, TX) with a size exclusion of 14000 g/mol for globular molecules. The OSG was obtained by drying with an LGJ-10 vacuum freeze-dryer (Sikuan Instrument Co. Ltd., Beijing, China) at −60 °C for 12 h and used for all subsequent experiments. The Fourier transform IR (FTIR) spectra of the products confirmed the substitution reaction. The IR spectra

Table 1. Weight-Average Molecular Weight (M_w), Degree of Substitution (DS), Critical Micelle Concentration (CMC), Size, ζ-Potential, and Polydispersity Index (PDI) of Octenylsuccinate Oat β-Glucan (OSG)[a,b]

sample	M_w[c] (10^4 g/mol)	DS	CMC (mg/mL)	size (nm)	ζ-potential (mV)	PDI
β-glucan	16.8	–	–	691.0 ± 10.5[a]	−8.7 ± 0.2[a]	0.459 ± 0.020[b]
OSG1	16.8	0.0080 ± 0.0005[c]	0.206 ± 0.006[a]	600.3 ± 19.3[b]	−11.5 ± 0.3[c]	0.474 ± 0.026[b]
OSG2	16.8	0.0172 ± 0.0025[b]	0.065 ± 0.003[c]	476.8 ± 14.2[c]	−12.5 ± 0.2[d]	0.558 ± 0.028[a]
OSG3	16.8	0.0387 ± 0.0018[a]	0.039 ± 0.002[d]	267.2 ± 7.5[d]	−13.7 ± 0.4[e]	0.528 ± 0.030[a,b]
OSG4	11.9	0.0085 ± 0.0007[c]	0.081 ± 0.004[b]	401.4 ± 10.1[e]	−10.9 ± 0.5[c]	0.443 ± 0.041[b]
OSG5	7.3	0.0076 ± 0.0010[c]	0.077 ± 0.004[b,c]	175.3 ± 8.6[f]	−9.6 ± 0.2[b]	0.293 ± 0.084[c]

[a]Values bearing different nonitalic superscript lowercase letters in the same column are significantly different ($P < 0.05$) by Tukey's HSD test. [b]2.5 mg/mL samples were used for the experiments on size, ζ-potential, and PDI. An aliquot solution of 100 mL of oat β-glucan (16.8×10^4 g/mol) or its hydrolysates (11.9×10^4 and 7.3×10^4 g/mol) was introduced into a reaction bulb. A 0.3 mL amount of 2-octen-1-ylsuccinic anhydride was added, and the mixture was incubated at 45 °C for 2 h under continuous stirring to obtain OSG1, OSG4, and OSG5. An aliquot solution of 100 mL of oat β-glucan (16.8×10^4 g/mol) was introduced into a reaction bulb. A 0.6 mL amount of 2-octen-1-ylsuccinic anhydride was added, and the mixture was incubated at 45 °C for 2 and 5 h under continuous stirring to obtain OSG2 and OSG3. [c]The molecular weight of soluble oat β-glucan was determined before chemical modification.

($500\ cm^{-1}$ to $4000\ cm^{-1}$, KBr disk method) were recorded by using a PerkinElmer Spectrum 2000 Fourier transform IR spectrometer (Shelton, CT) with a deuterated triglycine sulfate detector. Elemental analysis was conducted to determine the DS of OSG by using an Elementar CHNS analyzer (Vario EL III, Elementar Analysensysteme, Germany).[23]

OSG Micelles Preparation. OSG (50 mg) was dissolved in 20 mL of distilled water by heating at 100 °C for 2 min. The solution was cooled to room temperature when OSG was completely dissolved, and the volume was increased to 20 mL with distilled water. The obtained OSG micelles were used for TEM imaging, the measurement of micelle size and ζ-potential, and loading curcumin.

TEM. TEM was applied to characterize the appearance of OSG self-assembled micelles in aqueous solution.[24] A sample (2.5 mg/mL OSG1 solution, 3 μL) was dropped onto the carbon-coated grid and dried under ambient conditions overnight. To stain the micelles, phosphotungstic acid (PTA; 0.5 w/v %) solution (10 μL) was dropped onto the micelles for 2 min. A filter paper was then used to blot carefully the excess PTA solution. The grids were dried again under ambient conditions overnight. Imaging was performed on a JEOL JEM-2100 instrument (JEOL, Japan) at 200 kV equipped with a Gatan 94 Ultrascan 1k charge-coupled device camera.

Fluorescence Spectroscopy. A previously described pyrene 1:3 ratio method was adopted to determine the CMC of OSG.[25] A series of aqueous OSG solutions with varied concentrations (0.0004 mg/mL to 1.2 mg/mL) were prepared. The pH of these solutions was adjusted to 6.5 ± 0.2 by NaOH or HCl solution. Pyrene in ethanol (2×10^{-3} M) was then introduced into the aqueous OSG solution at a final concentration of 6×10^{-7} M. After intensive homogenization, the solution was stored overnight at room temperature. Fluorescence spectra were recorded on a Hitachi F-2500 fluorescence spectrophotometer (Hitachi, Japan) with a 10 mm path length quartz cuvette. In this system, pyrene was excited at 330 nm. The slit width was set to 10 nm for both excitation and emission. The fluorescence intensities in the emission spectra at ≈373 (I_1) and ≈384 nm (I_3) were measured. The I_1/I_3 quotient was defined as a pyrene 1:3 ratio value. CMC was determined by the intersection of the two straight lines drawn before and after the intersection point in the I_1/I_3 versus OSG concentration plots.[26]

Micelle Size and ζ-Potential. The size and ζ-potential of OSG micelles in aqueous solution were determined based on dynamic light scattering (DLS) by using a Zetasizer Nano ZS90 (Malvern Instruments Ltd., UK) equipped with a He−Ne laser (633 nm) and 90° collecting optics.[27] The results of size and ζ-potential were expressed as nm and mV. To study the influence of ionic strength (IS), 2.5 mg/mL OSG1 solutions (pH = 7) were prepared by the addition of NaCl to a final concentration of 0.1 to 0.5 M. To study the influence of pH, the pH values of 2.5 mg/mL OSG1 solutions (IS = 0 M) were adjusted to values ranging from 1.5 to 7.0 using small amounts of 0.1 to 5.0 M HCl or 0.1 NaOH. The influence of OSG concentration on micelle stability was also studied by dissolving 2.5, 2.0, 1.5, 0.5, and 0.2 mg OSG1 in 10 mL of distilled water (pH = 7 and IS = 0 M).

Loading Curcumin into OSG Micelles. Solid curcumin (5 mg) was added into a 10 mL OSG solution containing 25 mg of OSG1. Then, the solution was homogenized at 12 000 rpm for 1 min using a homogenizer (IKA T18 basic, IKA-Werke GmbH & Co., Staufen, Germany). To allow curcumin solubilization, the resulting suspension was continuously stirred at 25 °C for 48 h. Finally, excessive solid curcumin was removed from the suspension by centrifugation at 5600*g* for 20 min, and a curcumin-loaded OSG solution was obtained.

Quantitation of Curcumin in OSG Micelles. The loaded curcumin mass in the OSG solution was determined by HPLC.[28] Before conducting the analysis, the curcumin-loaded OSG solution was mixed with methanol (1:4, v/v) to extract curcumin. Mixtures were vortexed for 2 min and then centrifuged at 5600*g* for 10 min. Finally, the supernatants were filtered by a 0.45 μm filter (Nylon 66, China). HPLC analysis was performed on a reverse-phase Thermo BDS C18 column (250 mm × 4.6 mm i.d.) from Thermo Fisher Scientific Inc. (Waltham, MA) with a 5 μm particle diameter by using an LC-20A HPLC instrument equipped with a photodiode array detector (20A; Shimadzu, Japan) operated at 420 nm. A mixture of 0.2% (v/v) formic acid (solvent A) and acetonitrile (solvent B) was supplied as the mobile phase at a flow rate of 0.7 mL/min. The gradient was programmed as follows: starting composition, A:B, 65%:35% *v*/*v*; 0 to 10 min, % *v*/*v* of B increased from 35% to 65%; 10 to 15 min, % *v*/*v* of B increased from 65% to 70%; 15 to 20 min, % *v*/*v* of B decreased from 70% to 35%. Curcumin was quantified by an external calibration curve ($y = -7.4 \times 10^5 + 2.3 \times 10^5 x$, $R^2 = 0.9875$). The results were expressed as μg/mL. The curcumin loading capacity (CLC) of OSG was calculated by using the following equation:[29]

$$\text{curcumin loading capacity } (\mu g/mg) = \frac{\text{mass of loaded curcumin in 1 mL of OSG solution } (\mu g)}{\text{mass of used OSG in 1 mL of OSG solution (mg)}} \quad (1)$$

Statistical Analysis. Results were expressed as the mean with a standard deviation from at least three measurements. SPSS 19.0 was used to analyze the data. ANOVA was performed to determine the least significance at $P < 0.05$ by Tukey's HSD test.

RESULTS AND DISCUSSION

OSG Synthesis and Characterization. To investigate the effects of DS on the aqueous self-assembly behavior of OSG, OSG (M_w, 16.8×10^4 g/mol) with varied DS (OSG1, 0.0080; OSG2, 0.0172; OSG3, 0.0387) was used (Table 1). Oat β-glucan (OSG1, 16.8×10^4 g/mol) and its acid hydrolysates (OSG4, 11.9×10^4 g/mol; OSG5, 7.3×10^4 g/mol) with a comparative DS were also applied to evaluate the effects of oat

β-glucan M_w on the aqueous self-assembly behavior of OSG. HPSEC was used to characterize oat β-glucan M_w and hydrolyates, and FTIR spectroscopy was used to verify the substitution reaction (Figure 2). In all spectra, the broad band

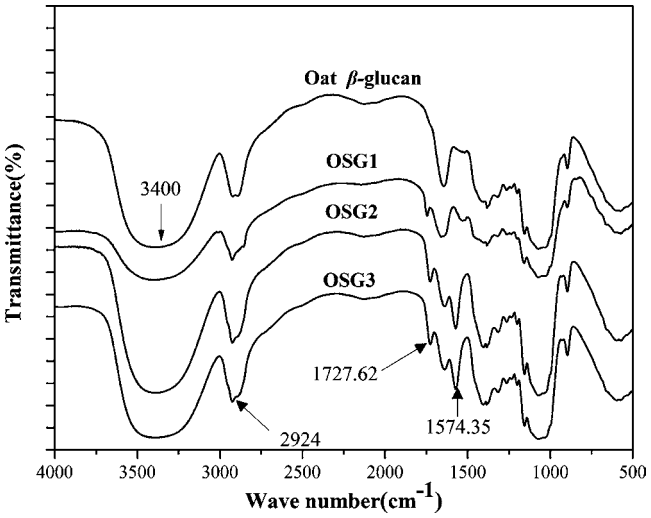

Figure 2. Infrared (IR) spectra of oat β-glucan and octenylsuccinate oat β-glucan (OSG).

stretch at approximately 3400 cm^{-1} is attributed to the hydrogen-bonded hydroxyls, and the band at ν = 2924 cm^{-1} is attributed to $-CH_2$ symmetrical stretching vibrations. In OSG spectra, newly derived peaks were observed at 1727 and 1574 cm^{-1}, which correspond to the OSG carbonyl group (−CO−) and the asymmetric stretch of vibration of the carboxylate ($RCOO^-$), respectively.[30,31] This evidence confirms the succession of intended chemical modifications. Similar observations are reported for OSA-modified starch.[32]

CMC of OSG. Figure 3 shows the fluorescence emission spectra of pyrene incorporated into OSG micelles in water at room temperature. Four characteristic peaks at 374, 380, 385, and 394.5 nm for pyrene appeared in the range of 360 to 420 nm, which agrees with the selected excitation wavelength of 330 nm for this system.[33] Given that pyrene senses a hydrophobic

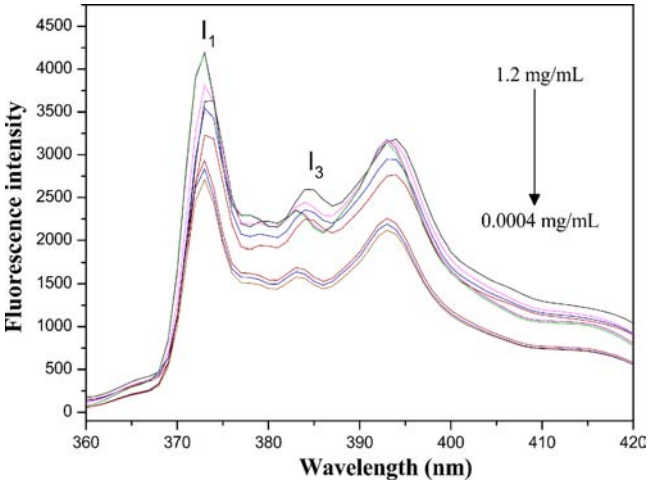

Figure 3. Emission spectra of pyrene (6.0×10^{-7} mg/mL) in octenylsuccinate oat β-glucan (OSG) solution as a function of OSG concentration (0.0004 to 1.2 mg/mL).

environment, the I_1/I_3 ratio is a sensitive indicator of the polarity of pyrene microenvironments. High and low I_1/I_3 ratios indicate polar and nonpolar environments, respectively. Thus, a decrease in I_1/I_3 ratio will indicate that pyrene is transferred from an aqueous media to less polar microdomains induced by OSG micellization. Figure 4 shows the plots of pyrene I_1/I_3 ratio versus the logarithm of OSG concentration. At low OSG concentrations, the I_1/I_3 ratio is approximately 1.80, which is similar to the value (1.87) measured in an aqueous environment (6.0×10^{-7} M of pyrene in phosphate buffer). An increase in OSG concentration results in a gradual decrease in I_1/I_3 ratio, thus suggesting the onset of OSG micellization. Theoretically, this finding indicates that OSG self-assemblies with hydrophobic cores are formed by the interactions between the octenylsuccinate groups, and pyrene is solubilized. High OSG concentrations result in increased pyrene incorporation into the hydrophobic cores.[34] The CMC of OSG varies from 0.039 mg/mL to 0.206 mg/mL. This result is similar to the values reported for (C_{17}, C_{15}, C_7)-acyl chitosan (0.002 mg/mL to 0.025 mg/mL), deoxycholic acid-modified chitosan (0.013 mg/mL to 0.075 mg/mL), and palmitoyl chitosan (0.002 mg/mL to 0.037 mg/mL).[26,35,36] The CMC values of OSGs are significantly lower than that of the low molecular weight surfactants (e.g., 2.5 mg/mL for sucrose fatty acid esters), indicating the stability of self-aggregates at dilute conditions.

The effects of the DS and M_w of oat β-glucan on the CMC values of OSG are summarized in Table 1. The comparisons of OSG1, OSG2, and OSG3 show the significant effect of the DS of OSG on its CMC. An increase in DS results in a sharp decrease in the CMC of OSG (0.206 mg/mL to 0.039 mg/mL). This finding is attributed to the enhanced hydrophobicity of OSG with its elevated DS. Therefore, hydrophobic interactions between octenylsuccinic groups influences the organization of a self-assembled network.[26,37,38]

The comparisons of OSG1, OSG4, and OSG5 show a sharp decrease in the CMC of OSG (from 0.206 mg/mL to 0.081 mg/mL) with a decrease in the M_w of oat β-glucan from 16.8×10^4 g/mol to 11.9×10^4 g/mol. A further decrease in the M_w of oat β-glucan does not result in a significant decrease in CMC. This finding is caused by the changes in rheology properties of the OSG solution and the molecular steric hindrance involved in the self-assembly. Acid hydrolysis significantly decreases the viscosity of the OSG solution; a decrease in viscosity aids the self-assembly.[39] Kim[40] reported that the high molecular weight of glycol chitosan backbone in glycol chitosan−deoxycholic acid conjugates significantly hampered the effective association of hydrophobic deoxycholic acids.

Morphology and Size of OSG Self-Assembly. The morphological characteristic of the OSG1 micelle is shown in Figure 5. The stained micelles appear as dark objects against the light background of the amorphous carbon substrate and are separated well from each other. OSG1 micelles under neutral conditions have a spherical structure with a size of approximately 600 nm. Table 1 indicates that the PDI of OSG self-assembly increased from 0.293 to 0.474 with the increase of OSG M_w from 7.3×10^4 to 16.8×10^4 g/mol. The OSG with high M_w is likely to form self-assemble with different dimensions, leading to more heterogeneity. A significant increase in the PDI of OSG was also observed with the increase of DS from 0.0080 to 0.172. However, with a further increase of DS to 0.0387, the PDI did not increase significantly. Higher PDI of OSG at higher DS may ascribe to the higher

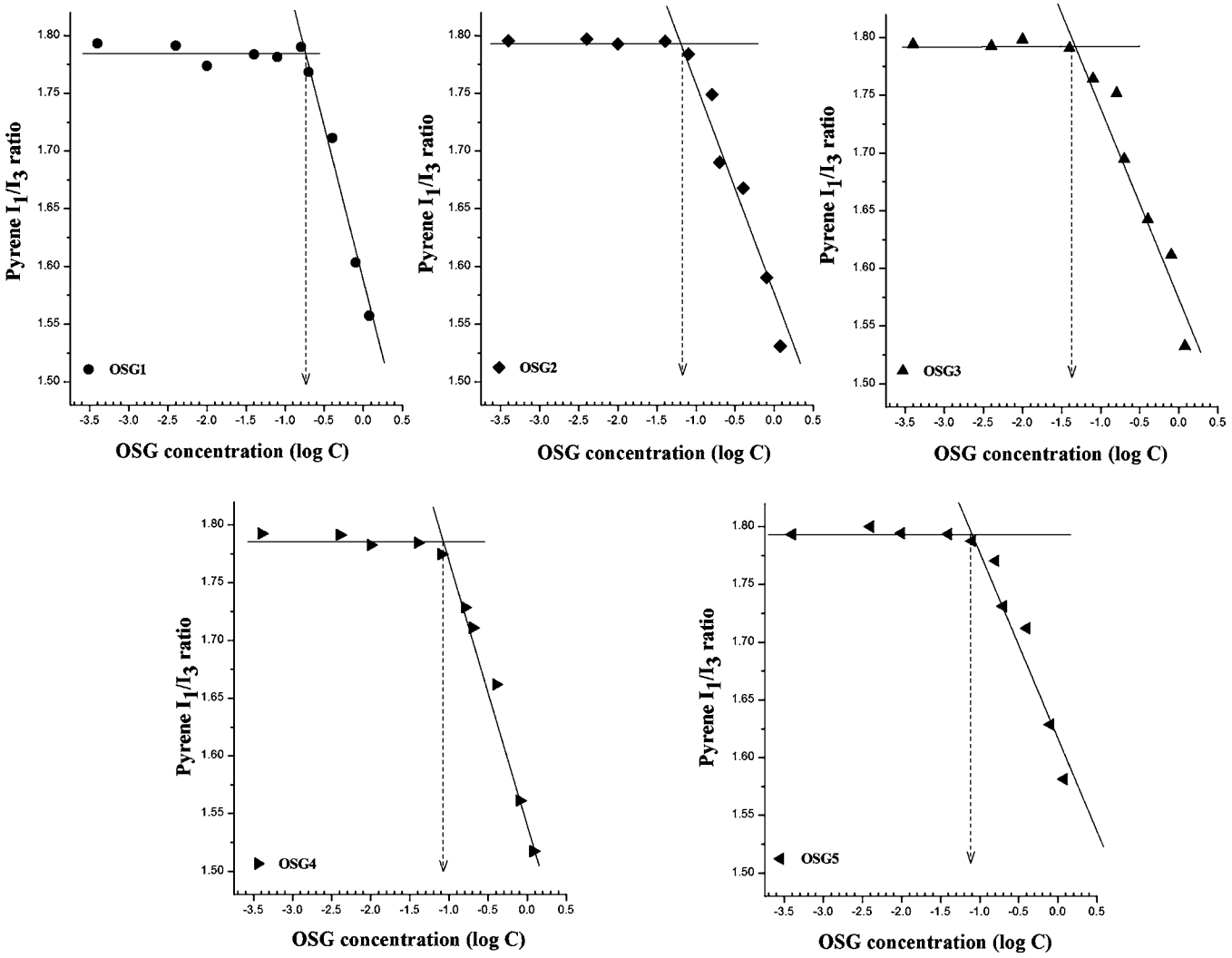

Figure 4. Plots of pyrene I_1/I_3 ratio versus the logarithm of different concentration of octenylsuccinate oat β-glucan (OSG) with different degrees of substitution (DS) and molecular weights of oat β-glucan (M_w).

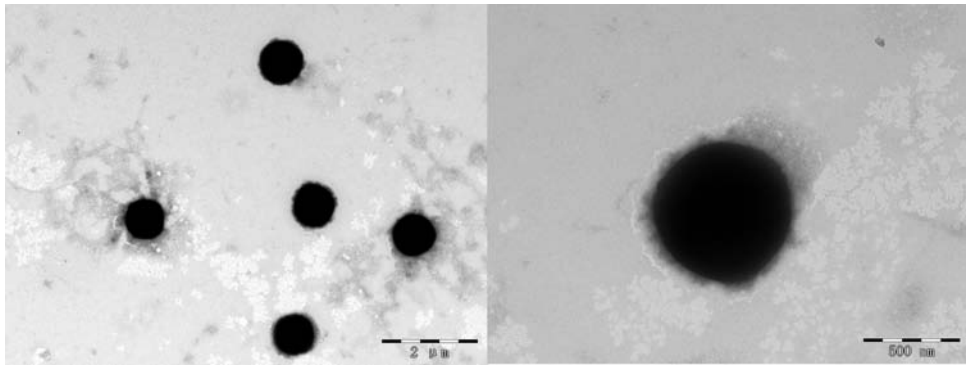

Figure 5. Transmission electron micrograph (TEM) of octenylsuccinate oat β-glucan (OSG) micelles.

amount of carboxyl groups, which leads to stronger intramolecular repulsion, making the OSG chain stretch and resulting in the higher PDI. The self-assembly size is one of the most significant determinants for the transparency and stability of OSG solutions, as well as the loading capacity and bioavailability of loaded chemicals.[41,42] Table 1 shows that both the DS and M_w of oat β-glucan significantly affects the size of self-assemblies. An increase in DS significantly decreases the size of the self-assemblies. This finding indicates that compact self-assemblies are formed with high-DS OSGs. Similar results have been reported for oleoyl alginate ester, octadecyl hyaluronic acid, and palmitoyl chitosan.[36,43,44] This phenomenon can be ascribed to the strong intra- and intermolecular hydrophobic interactions among octenylsuccinic groups, thus causing the hydrophobic substituent groups to self-assemble and form a dense core. For the M_w of oat β-glucan, a high M_w is

accompanied by large self-assemblies. Thus, a decrease in the M_w of oat β-glucan decreases micelle size. This result can be attributed to two related factors. First, lower molecular weight polymers have lower steric hindrances and higher flexibilities, which facilitate compaction in self-assemblies, compared with that of higher molecular weight polymers. Second, a decrease in the M_w of polymer amphiphiles decreases the vesicle curvature of self-assemblies.[45]

In addition to the structural parameters of OSG, environmental factors also affect the size of formed self-assemblies. The effect of OSG concentration on the size of OSG self-assemblies are shown in Figure 6A with OSG1 as the model substrate. At an OSG concentration equal to the CMC (0.2 mg/mL), the size of the micelles is 325 nm. An increase in OSG concentration results in a sharp increase in particle size and then reaches a plateau (540 nm) at concentrations above 1.5 mg/mL. A similar increase has been reported for chitosan−glutathione conjugate nanoparticles.[46] The increase in particle size is due to the increased viscosity of the OSG solution resulting from high concentrations. Figure 6B shows the effects of ionic strength on the size of OSG self-assemblies. When the NaCl concentration ranges from 0 to 0.3 M, micelle size decreases from 600 to 475 nm. However, a further increase in NaCl concentrations above 0.3 M insignificantly affects the micelle size. Electrolytes (Na^+) screen the electrostatic repulsion of negative charges ($-COO^-$) in the β-glucan backbone, thus resulting in size reduction.[26] Figure 6C shows the effect of pH on the micelle size. A low pH corresponds to small micelle sizes. This finding is attributed to the pH dependence of ionization state carboxyls in substituent groups. The ratio of deprotonated/protonated carboxyl groups (COO^-/COOH) increases with the increasing pH of the OSG solution. Thus, the repulsion among individual OSG molecules caused by the deprotonated carboxyl groups at high pH reduces particle aggregation and increases self-assembly size. All carboxyl groups are fully deprotonated when the pH is above 5.5, and the size of self-assemblies is independent of the pH of the OAG solution.

ζ-Potential of OSG Self-Assembly. ζ-Potential analysis was performed to obtain information on the surface properties of the micelles. ζ-Potential is an indicator for the long-term stability of particulate systems. If particles in a suspension have large ζ-potential values, such particles will repel each other and will not aggregate. This phenomenon is reflected by the stability of the suspension. However, if the particles have low ζ-potential values (close to zero), such particles will aggregate, thus destabilizing the suspension.[47] OSG micelles present a negative charge, which is possibly caused by the presence of ionized carboxyl groups at the micelle surface (Table 1). The absolute ζ-potential of self-assemblies increases with the increasing DS of OSG compared with OSG1, OSG2, and OSG3. A higher DS leads to a higher absolute ζ-potential, thus suggesting that large amounts of OS groups cause high surface charge density.[48,49] Although the absolute ζ-potentials insignificantly differ between OSG self-assemblies with β-glucan M_w of 16.8×10^4 and 11.9×10^4 g/mol, such absolute ζ-potentials are higher than the absolute ζ-potentials of OSG self-assemblies with a β-glucan M_w of 7.3×10^4 g/mol. At the equivalent DS, a decrease in M_w of β-glucan may decrease the surface OSA group density of OSG micelle, which finally causes the lower absolute ζ-potential. Figure 6A presents the ζ-potential of micelles as a function of OSG concentration. In a concentration range of 0.2 mg/mL to 2.5 mg/mL, the absolute ζ-potential of

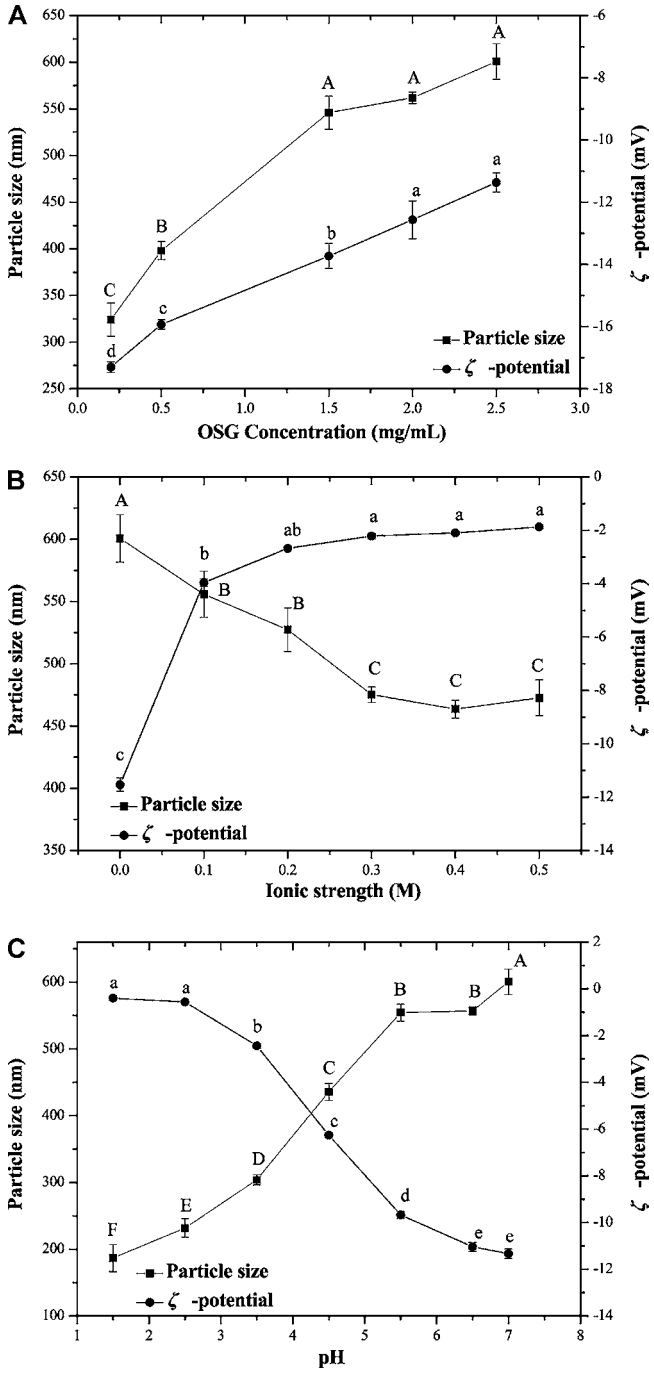

Figure 6. Effects of octenylsuccinate oat β-glucan (OSG) concentration (A), ionic strength (B), and pH (C) on the size and ζ-potential of micelles. Values are given as the mean of three independent experiments, and error bars represent the SD. Different lower case letters indicate a significant difference ($P < 0.05$).

micelles decreases with OSG concentration. The average particle spacing becomes very small at high concentrations. With such small average particle spacing at high concentrations, overlapping electrical double layers may have an influence.[50] Thus, the lower absolute ζ-potential is accompanied by higher OSG concentration. The introduction of 0.1 M NaCl results in a sharp change in the ζ-potential of OSG micelles from −11.5 mV to −1.9 mV (Figure 6B). However, a further increase in NaCl concentration presents statistically significant results but insignificantly affects ζ-potential. The introduction of NaCl

increases the ionic strength and reduces the thickness of the electric double layer of micelles, thus leading to the decrease of ζ-potential.[10] Figure 6C illustrates the effects of pH on the ζ-potential of OSG micelles. The increase in pH is accompanied by an elevated ζ-potential of OSG micelles. When the pH reaches 5.5, a ζ-potential of approximately −9.67 mV is obtained for formed micelles. The increase in absolute ζ-potential can be attributed to the ionization state of surface carboxyl groups on micelles. A high pH increases deprotonated and negatively charged carboxyl groups on the micelle surface. These charged carboxyl groups are responsible for the increase in absolute ζ-potential.[51]

Application of OSG Self-Assemblies. Curcumin was selected as a model chemical because of its poor water solubility to test the solubilization capacity of lipophilic food components in OSG micelles. Free curcumin appears as insoluble particulates (Figure 7) because of its low solubility of 11 ng/mL. The loaded curcumin concentration in aqueous 2.5 mg/mL OSG1 solution was measured at 9.68 μg/mL by HPLC, which was 880 fold of its solubility in water. Therefore, OSG self-assemblies can be used as a vehicle to encapsulate and deliver a variety of lipophilic food components. The self-assemblies of biomacromolecule derivatives including hydrophobically modified starch (OSA starch), β-casein (BC), hydroxypropyl-β-cyclodextrin (HP-β-CD), and hydroxypropyl-γ-cyclodextrin (HP-γ-CD) enhance the solubility of curcumin.[52−54] To compare the solubilization capacity of different polymers, a term of curcumin loading capacity (CLC) was introduced, which was defined as the amount of curcumin (μg) solubilized by 1 mg of polymer. The CLCs of OSA starch, BC, HP-β-CD, and HP-γ-CD are 1.8, 2.8, 1.3, and 3.4 μg/mg, respectively, which are lower than those of our polymer (OSG1, 3.9 μg/mg). This result suggests that OSG self-assemblies are very efficient in solubilizing curcumin. This study reported the synthesis of a hydrophobic oat β-glucan polymer. Self-assembly in aqueous OSG solutions show the formation of spherical micelles with particle sizes ranging from 175 to 600 nm. The hydrophobic interaction among octenylsuccinic groups facilitates the assembly process. The DS, oat β-glucan M_w, NaCl, pH, and OSG concentration affect micelle size. Higher DS, oat β-glucan M_w, and pH values result in higher absolute ζ-potential values, which aid the stability of the OSG suspension. On the contrary, the addition of NaCl significantly decreases the absolute ζ-potential and the stability of the OSG suspension. The sensitivity of OSG micelles to pH and ionic strength is due to the virtual changes in the ionization state of carboxyl groups (COO^-/COOH). This study confirms that OSG micelles present high efficiency in solubilizing curcumin in terms of polymer loading capacity. Further studies on the current topic are required to address the following aspects. First, information on OSG micelle microstructure is important to the technique functionality. Second, the effects of OSG micelle structure on CLC are vital in optimizing the design of OSG micelles. Third, the stability and physiochemical properties of the curcumin-loaded OSG is important to its further application.

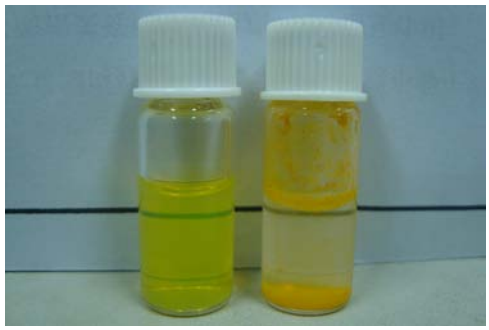

Figure 7. Photographic images of curcumin in the solution containing 2.5 mg/mL octenylsuccinate oat β-glucan (OSG) micelles.

AUTHOR INFORMATION

Corresponding Author

*Tel: +86 23 68 25 9 02. Fax: +86 23 68 25 19 47. E-mail: zhaogh@swu.edu.cn.

Funding

This study was financially supported by the National Natural Science Foundation of China (31371737).

Notes

The authors declare no competing financial interest.

ACKNOWLEDGMENTS

The authors thank Prof. C. X. Guo and Dr. H. Y. Cao for their kind help in TEM imaging and the measurement of size and ζ-potential.

REFERENCES

(1) Whitesides, G. M.; Grzybowski, B. Self-assembly at all scales. *Science* **2002**, *295*, 2418−2421.

(2) Goncalves, G.; Martins, J. A.; Gama, F. M. Self-assembled nanoparticles of dextrin substituted with hexadecanethiol. *Biomacromolecules* **2007**, *8*, 392−398.

(3) Wang, C.; Wang, Z. Q.; Zhang, X. Amphiphilic building blocks for self-Assembly: from amphiphiles to supra-amphiphiles. *Acc. Chem. Res.* **2012**, *45*, 608−618.

(4) Nishiura, H.; Sugimoto, K.; Akiyama, K.; Musashi, M.; Kubota, Y.; Yokoyama, T.; Yamashita, Y.; Kuriki, T.; Yamaguchi, Y. A novel nano-capsule of α-lipoic acid as a template of core-shell structure constructed by self-assembly. *J. Nanomed. Nanotechnol.* **2013**, *4*, 155.

(5) Bisht, S.; Feldmann, G.; Soni, S.; Ravi, R.; Karikar, C.; Maitra, A. Polymeric nanoparticle-encapsulated curcumin ("nanocurcumin"): a novel strategy for human cancer therapy. *J. Nanobiotechnol.* **2007**, *5*, 1−18.

(6) Le, T. T. D.; La, T. H.; Le, T. M. P.; Nguyen, T. M. H.; Le, Q. H. Docetaxel and curcumin-containing poly(ethylene glycol)-block-poly(ε-caprolactone) polymer micelles. *Adv. Nat. Sci.: Nanosci. Nanotechnol.* **2013**, *4*, 025006.

(7) Miller, T.; Breyer, S.; Colen, G. V.; Mier, W.; Haberkorn, U. Premature drug release of polymeric micelles and its effects on tumor targeting. *Int. J. Pharm.* **2013**, *445*, 117−124.

(8) Chen, W.; Zhong, P.; Meng, F.; Cheng, R.; Deng, C.; Feijen, J.; Zhong, Z. Redox and pH-responsive degradable micelles for dually activated intracellular anticancer drug release. *J. Controlled Release* **2013**, *169*, 171−179.

(9) Solmatin, S. V.; Bronich, T. K.; Bargar, T. W.; Eisenberg, A.; Kabanov, V. A.; Kabanov, A. V. Environmentally Responsive Nanoparticles from Block Ionomer Complexes: Effects of pH and Ionic Strength. *Langmuir* **2003**, *19*, 8069−8076.

(10) Jin, F.; Li, J. F.; Ye, X. D.; Wu, C. Effects of pH and ionic strength on the stability of nanobubbles in aqueous solutions of α-cyclodextrin. *J. Phys. Chem. B* **2007**, *111*, 11745−11749.

(11) Lee, K. Y.; Jo, W. H.; Kwon, I. C.; Kim, Y. H.; Jeong, S. Y. Structural determination and interior polarity of self-aggregates prepared from deoxycholic acid-modified chitosan in water. *Macromolecules* **1998**, *31*, 378−383.

(12) Besheer, A.; Hause, G.; Kressler, J.; Mäder, K. Hydrophobically modified hydroxyethyl starch: synthesis, characterization, and aqueous

self-assembly into nano-sized polymeric micelles and vesicles. *Biomacromolecules* **2007**, *8*, 359−367.
(13) Song, Y. B.; Zhang, L. Z.; Gan, W. P.; Zhou, J. P.; Zhang, L. N. Self-assembled micelles based on hydrophobically modified quaternized cellulose for drug delivery. *Colloids Surf. B* **2011**, *83*, 313−320.
(14) Goncalves, G.; Martins, J. A.; Gama, F. M. Self-assembled nanoparticles of dextrin substituted with hexadecanethiol. *Biomacromolecules* **2007**, *8*, 392−398.
(15) Li, Y. Y.; Chen, X. G.; Cha, D. S.; Park, H. J.; Lee, C. M. Effect of the molecular mass and degree of substitution of oleoylchitosan on the structure, rheological properties, and formation of nanoparticles. *J. Agric. Food Chem.* **2007**, *55*, 4842−4847.
(16) Tang, D. W.; Yu, S. H.; Ho, Y. C.; Huang, B. Q.; Tsai, G. J.; Hsieh, H. Y.; Sung, H. W.; Mi, F. L. Characterization of tea catechins-loaded nanoparticles prepared from chitosan and an edible polypeptide. *Food Hydrocolloids* **2013**, *30*, 33−41.
(17) Wang, X. H.; Tian, Q.; Wang, W.; Zhang, C. N.; Wang, P.; Yuan, Z. In vitro evaluation of polymeric micelles based on hydrophobically-modified sulfated chitosan as a carrier of doxorubicin. *J. Mater Sci.: Mater. Med.* **2012**, *23*, 1663−1674.
(18) Das, R. K.; Kasoju, N.; Bora, U. Encapsulation of curcumin in alginate-chitosan-pluronic composite nanoparticles for delivery to cancer cells. *Nanomedicine (N. Y., NY, U. S.)* **2010**, *6*, 153−160.
(19) Wu, Z.; Ming, J.; Gao, R. P.; Wang, Y. X.; Liang, Q.; Zhao, G. H. Characterization and antioxidant activity of the complex of tea polyphenols and oat β-glucan. *J. Agric. Food Chem.* **2011**, *59*, 10737−10746.
(20) Tosh, S. M.; Wood, P. J.; Wang, Q.; Weisz, J. Structural characteristics and rheological properties of partially hydrolyzed oat β-glucan: The effects of molecular weight and hydrolysis method. *Carbohydr. Polym.* **2004**, *55*, 425−436.
(21) Lazaridou, A.; Biliaderis, C. G.; Izydorczyk, M. S. Molecular size effects on rheological properties of oat β-glucans in solution and gels. *Food Hydrocolloids* **2003**, *17*, 693−712.
(22) Yusoff, A.; Murray, B. S. Modified starch granules as particle-stabilizers of oil-in-water emulsions. *Food Hydrocolloids* **2011**, *25*, 42−55.
(23) Shin, M. S; Lee, S.; Lee, K. Y.; Lee, H. G. Structural and biological characterization of aminated-derivatized oat β-glucan. *J. Agric. Food Chem.* **2005**, *53*, 5554−5558.
(24) Zhu, Y. Q.; Liu, Li.; Du, J. Z. Probing into Homopolymer Self-Assembly: How Does Hydrogen Bonding Influence Morphology? *Macromolecules* **2013**, *46*, 194−203.
(25) Aguiar, J.; Carpena, P.; Molina-Bolívar, J. A.; Ruiz, C. C. On the determination of the critical micelle concentration by the pyrene 1:3 ratio method. *J. Colloid Interface Sci.* **2003**, *258*, 116−122.
(26) Lee, K. Y.; Jo, W. H.; Kwon, I. C.; Kim, Y. H.; Jeong, S. Y. Physicochemical characteristics of self-aggregates of hydrophobically modified chitosans. *Langmuir* **1998**, *14*, 2329−2332.
(27) Luo, Y. C.; Teng, Z.; Wang, Q. Development of zein nanoparticles coated with carboxymethyl chitosan for encapsulation and controlled release of vitamin D3. *J. Agric. Food Chem.* **2012**, *60*, 836−843.
(28) Jayaprakasha, G. K.; Rao, L. J. M.; Sakariah, K. K. Improved HPLC method for the determination of curcumin, demethoxycurcumin, and bisdemethoxycurcumin. *J. Agric. Food Chem.* **2002**, *50*, 3668−3672.
(29) Gou, P. F.; Zhu, W. P.; Shen, Z. Q. Synthesis, self-assembly, and drug-loading capacity of well-defined cyclodextrin-centered drug-conjugated amphiphilic A14B7 miktoarm star copolymers based on poly(ε-caprolactone) and poly(ethylene glycol). *Biomacromolecules* **2010**, *11*, 934−943.
(30) Marcazzan, M.; Vianello, F.; Scarpa, M.; Rigo, A. An ESR assay for α-amylase activity toward succinylated starch, amylose and amylopectin. *J. Biochem. Biophys. Methods* **1999**, *38*, 191−202.
(31) Nagaoka, S.; Tobata, H.; Takiguchi, Y.; Satoh, T.; Sakurai, T.; Takafuji, M.; Ihara, H. Characterization of cellulose microbeads prepared by a viscose-phase-separation method and their chemical modification with acid anhydride. *J. Appl. Polym. Sci.* **2005**, *97*, 149−157.
(32) He, J. H.; Liu, J.; Zhang, G. Y. Slowly Digestible Waxy Maize Starch Prepared by Octenyl Succinic Anhydride Esterification and Heat−Moisture Treatment: Glycemic Response and Mechanism. *Biomacromolecules* **2008**, *9*, 175−184.
(33) Wang, Y. S.; Liu, L. R.; Weng, J.; Zhang, Q. Q. Preparation and characterization of self-aggregated nanoparticles of cholesterol-modified *O*-carboxymethyl chitosan conjugates. *Carbohydr. Polym.* **2007**, *69*, 597−606.
(34) Vieira, N. A. B.; Moscardini, M. S.; de Oliveira Tiera, V. A.; Tiera, M. J. Aggregation behavior of hydrophobically modified dextran in aqueous solution: A fluorescence probe study. *Carbohydr. Polym.* **2003**, *53*, 137−143.
(35) Jiang, G. B.; Quan, D. P.; Liao, K. R.; Wang, H. H. Preparation of polymeric micelles based on chitosan bearing a small amount of highly hydrophobic groups. *Carbohydr. Polym.* **2006**, *66*, 514−520.
(36) Jiang, G. B.; Quan, D. P.; Liao, K. R.; Wang, H. H. Novel polymer micelles prepared from chitosan grafted hydrophobic palmitoyl groups for drug delivery. *Mol. Pharm.* **2006**, *3*, 152−160.
(37) Gong, J.; Huo, M. R.; Zhou, J. P.; Zhang, Y.; Peng, X. L.; Yu, D.; Zhang, H.; Li, J. Synthesis, characterization, drug-loading capacity and safety of novel octyl modified serum albumin micelles. *Int. J. Pharm.* **2009**, *376*, 161−168.
(38) Li, Y. Y.; Chen, X. G.; Liu, C. S.; Cha, D. S.; Park, H. J.; Lee, C. M. Effect of the molecular mass and degree of substitution of oleoylchitosan on the structure, rheological properties, and formation of nanoparticles. *J. Agric. Food Chem.* **2007**, *55*, 4842−4847.
(39) Johansson, L.; Virkki, L.; Anttila, H.; Esselström, H.; Tuomainen, P.; Sontag-Strohm, T. *Food Chem.* **2006**, *97*, 71−79.
(40) Kim, K.; Kwon, S.; Park, J. H.; Chung, H.; Jeong, S. Y.; Kwon, I. C.; Kim, I. S. Physicochemical characterizations of self-assembled nanoparticles of glycol chitosan−deoxycholic acid conjugates. *Biomacromolecules* **2005**, *6*, 1154−1158.
(41) Song, C.; Labhasetwar, V.; Cui, X.; Underwood, T.; Levy, R. J. Arterial uptake of biodegradable nanoparticles for intravascular local drug delivery: Results with an acute dog model. *J. Controlled Release* **1998**, *54*, 201−211.
(42) Desai, M. P.; Labhasetwar, V.; Amidon, G. L.; Levy, R. J. Gastrointestinal uptake of biodegradable microparticles: Effect of particle size. *Pharm. Res.* **1996**, *13*, 1838−1845.
(43) Li, Q.; Liu, C. G.; Huang, Z. H.; Xue, F. F. Preparation and characterization of nanoparticles based on hydrophobic alginate derivative as carriers for sustained release of vitamin D_3. *J. Agric. Food Chem.* **2011**, *59*, 1962−1967.
(44) Liu, Y. H.; Sun, J.; Cao, W.; Yang, J. H.; Lian, H.; Li, X.; Sun, Y. H.; Wang, Y. J.; Wang, S. L.; He, Z. G. Dual targeting folate-conjugated hyaluronic acid polymeric micelles for paclitaxel delivery. *Int. J. Pharm.* **2011**, *421*, 160−169.
(45) Wang, W.; McConaghy, A. M.; Tetley, L.; Uchegbu, I. F. Controls on polymer molecular weight may be used to control the size of palmitoyl glycol chitosan polymeric vesicles. *Langmuir* **2001**, *17*, 631−636.
(46) Koo, S. H.; Lee, J. S.; Kim, G. H.; Lee, H. G. Preparation, characteristics, and stability of glutathione-loaded nanoparticles. *J. Agric. Food Chem.* **2011**, *59*, 11264−11269.
(47) Jacobs, C.; Müller, R. H. Production and characterization of a budesonide nanosuspension for pulmonary administration. *Pharm. Res.* **2002**, *19*, 189−194.
(48) Scheffler, S. L.; Wang, X.; Huang, L.; San-Martin Gonzalez, F.; Yao, Y. Phytoglycogen octenylsuccinate, an amphiphilic carbohydrate nanoparticle, and ε-polylysine to improve lipid oxidative stability of emulsions. *J. Agric. Food Chem.* **2009**, *58*, 660−667.
(49) Lee, C. T.; Huang, C. P.; Lee, Y. D. Preparation of amphiphilic poly(L-lactide)-graft-chondroitin sulfate copolymer self-aggregates and its aggregation behavior. *Biomacromolecules* **2006**, *7*, 1179−1186.
(50) Kaszuba, M.; Corbett, J.; Watson, F. M.; Jones, A. High-concentration zeta potential measurements using light-scattering techniques. *Philos. Trans. R. Soc., A* **2010**, *368*, 4439−4451.

(51) Skaat, H.; Chen, R.; Grinberg, I.; Margel, S. Engineered polymer nanoparticles containing hydrophobic dipeptide for inhibition of amyloid-β fibrillation. *Biomacromolecules* **2012**, *13*, 2662−2670.
(52) Yu, H. L.; Huang, Q. R. Enhanced in vitro anti-cancer activity of curcumin encapsulated in hydrophobically modified starch. *Food Chem.* **2011**, *119*, 669−674.
(53) Esmaili, M.; Ghaffari, S. M.; Moosavi-Movahedi, Z.; Atri, M. S.; Sharifizadeh, A.; Farhadi, M.; Yousefi, R.; Chobert, J.-M.; Haertlé, T.; Moosavi-Movahedi, A. A. Beta casein-micelle as a nano vehicle for solubility enhancement of curcumin; food industry application. *LWT–Food Sci. Technol.* **2011**, *44*, 2166−2172.
(54) Baglole, K. N.; Boland, P. G.; Wagner, B. D. Fluorescence enhancement of curcumin upon inclusion into parent and modified cyclodextrins. *J. Photochem. Photobiol., A* **2005**, *173*, 230−237.